

Chapter 6

Electrides and Their High-Pressure Chemistry

Xiao Dong and Artem R. Oganov

Abstract Recently, electrides were discovered in many systems (especially those containing alkali and alkali earth metals) at high pressures. An electride can be defined as an ionic compound where the role of an anion is played by a strongly localized electron density. High-pressure emergence of electrides is due to the Pauli expulsion of valence electrons from the core, while some electrides are better described as originating from multicenter covalent bonds. Not being bound directly to a nucleus, these localized electrons are chemically active, making electrides the strongest reducing agents known, able to interact even with such an extremely inert element as helium.

The Discovery of Electrides

In classical chemical systems, electron density is peaked on nuclei. However, in the 1970–1980s, a new type of compounds was established, in which bare electrons, not bound to any particular nucleus, are concentrated in the interstitial space and behave as anions. Such compounds were named electrides.

X. Dong (✉)

Center for High Pressure Science and Technology Advanced Research,
Beijing 100193, China
e-mail: xiao.dong@hpstar.ac.cn

A.R. Oganov

Skolkovo Innovation Center, Skolkovo Institute of Science and Technology,
3 Nobel Street, Moscow 143026, Russia
e-mail: a.oganov@skoltech.ru

A.R. Oganov

State University of New York, Stony Brook, NY 11794-2100, USA

A.R. Oganov

Moscow Institute of Physics and Technology, 9 Institutskiy Lane, Dolgoprudny,
Moscow Region 141700, Russia

A.R. Oganov

International Center for Materials Design, Northwestern Polytechnical University,
Xi'an 710072, China

© Springer International Publishing AG 2017

G.G.N. Angilella and A. La Magna (eds.), *Correlations in Condensed Matter under Extreme Conditions*, DOI 10.1007/978-3-319-53664-4_6

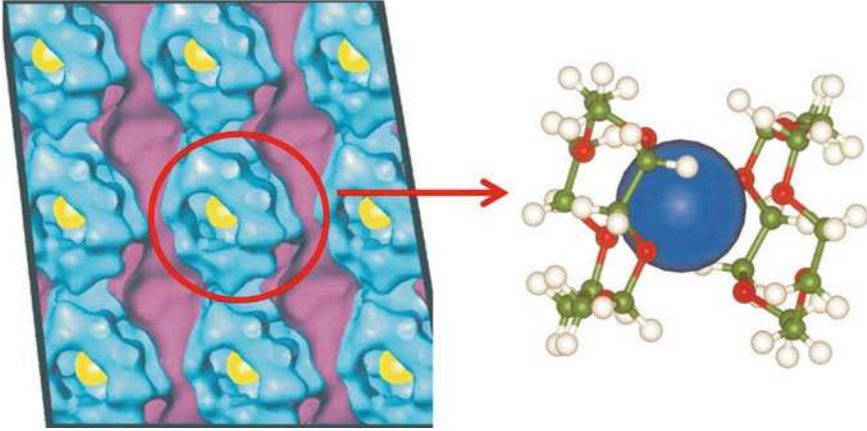


Fig. 6.1 Structure of the organic electride $\text{Cs}^+(15\text{-crown-5})_2e^-$. Electron-trapping cavities and channels are shown in *pink*, 15-crown-5 molecules in *blue*, and cesium cations in *yellow*. Inset shows the ball-and-stick representation of the $\text{Cs}^+(15\text{-crown-5})_2$ “sandwich,” with the Cs^+ ion drawn to scale [1] (color figure online)

The first clear report of an electride we could find dates back to 1981 [2], followed by many other discoveries of chemically complex compounds (at first, only organic, but then also inorganic [3]). In 1990, Dye [1, 4, 5] discovered that an organic crown ether or cryptand can trap electrons as counterions, in alkali metal complexes, such as $\text{Cs}^+(18\text{-crown-6})_2e^-$ or $\text{Cs}^+(15\text{-crown-5})_2e^-$. In such electrides as shown in Fig. 6.1, the localized electrons are usually single electrons occupying the cavities, and there is a weak spin–spin interaction between electrons occupying neighboring cavities. So, electrides known at normal pressure are paramagnetic or antiferromagnetic.

Since high pressure favors spin pairing, such spin-polarized electrides will obviously give way to spin-paired electrides under compression. Another insight into the nature of high-pressure electrides comes from a quantum-mechanical consideration of the interaction between valence and core electrons.

In 2008, Rousseau and Ashcroft [6] modeled the effects of core electrons as a hard potential $v(r) = V_0\theta(r_c - r)$, where r_c is the ionic radius, θ is the Heaviside step function and V_0 a hard screening potential. Using this potential, they wrote the Hamiltonian and the Schrödinger equation:

$$H(r) = -\frac{\hbar^2}{2m}\nabla^2 + \sum_R v(r - R), \quad (6.1a)$$

$$H\varphi = E\varphi, \quad (6.1b)$$

where R is the position of nucleus. To consider the effect of compression, they also employed an average radius of ions, $r_s = \sqrt[3]{3\Omega/4\pi N}$, where N is the number of atoms and Ω the volume. In this way, the parameter r_c/r_s can describe the compression ratio.

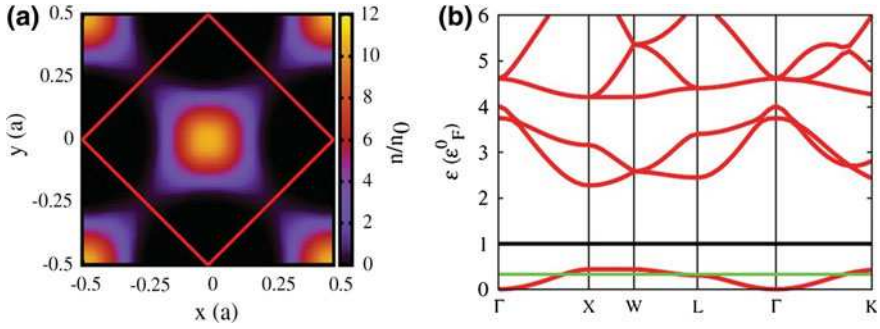


Fig. 6.2 Electronic properties calculated from Eq. (6.1b) with $r_c/r_s = 0.7$. **a** Electron density in the $z = 0$ plane. **b** Band structure (eigenvalue spectrum) for excluding spheres. The Fermi energy (green line) and the free electron Fermi energy (black line) are indicated [6] (color figure online)

Solving numerically the Schrödinger’s equation for the face-center cubic (fcc) structure, they found that when $r_c/r_s > 0.5$, the wave function will deviate significantly from the nearly free electron gas behavior and localize in the interstitial regions (Fig. 6.2a). In the band structure, the band width decreases with compression, which means the electrons are more localized (Fig. 6.2b). Already this oversimplified model gives an enlightening idea that electropositive atoms at strong compression may experience band narrowing, interstitial localization of valence electrons, and metal–insulator transition. The first anticipation of demetallization of alkali metals under pressure came from Professor Pucci’s group in 1997 [7], although not through the electrider mechanism.

Then, Ma and Oganov [8] found a true high-pressure electrider, transparent $hP4$ phase of sodium. In the high-pressure experiment, metallic sodium transformed under compression first to a poorly metallic incommensurate $tI19$ phase (black at 156 GPa, Fig. 6.3a) and then to the transparent phase $hP4$. In the $hP4$ structure, there are two kinds of Na atoms, Na1 and Na2, in total four atoms of Na and two interstitial sites with electron localization in the unit cell. Each interstitial site contains an electron pair, and the chemical formula can be written as $\text{Na}_2(2e)$. From structural geometry, one could imply pd and pd^2 hybridizations for Na1 in the octahedral sites and Na2 in the triangular prismatic coordination, respectively (Fig. 6.3b). It has a wide band gap—for example, GW calculations predict the band gap to be over 6 eV at 600 GPa, which implies a colorless transparent insulator.

Similar electrideres were also found for Li [9–12]. However, lithium atom has two differences from sodium: (1) the core radius (i.e., the ionic Li^+ radius, 0.76 Å) is much smaller than its covalent radius (1.28 Å) and van der Waals radius (1.82 Å). This means Li is quite compressible and easy to get into the electrider state—compared with Na (which becomes an electrider at pressures ~ 200 GPa), Li only needs 60 GPa to get into the semiconducting phase $C2cb-40$ [10]. (2) Li is much smaller than Na, thus the interstitial electrons are localized in a smaller space and nearer to each other, which means that electrons can more easily tunnel from one interstitial site to

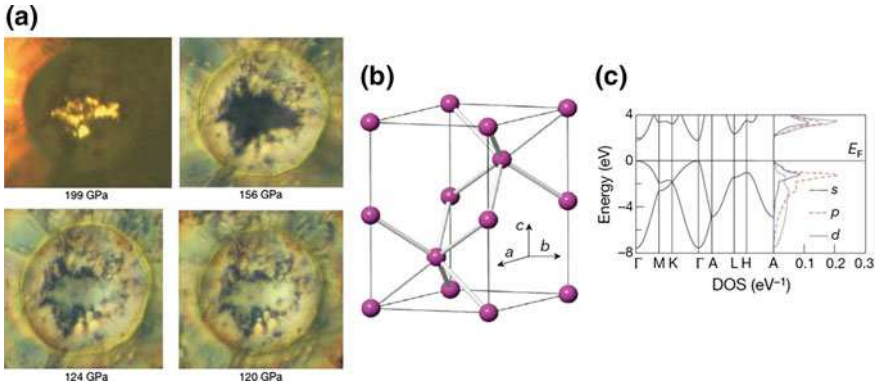


Fig. 6.3 **a** Photographs of the Na sample taken under pressure in the diamond anvil cell (DAC), showing an optically transparent sample at 199 GPa. **b** Crystal structure of *hP4*-Na (space group *P6₃/mmc*). **c** Band structure and partial densities of states (DOS) at 300 GPa. From Ref. [8]

another, and over the potential barrier formed by the repulsion from core electrons. As a result, the electrider state is sensitive and easy to break: e.g., the band gap is quite small (0.8 eV) and the external pressure causes a phase transition to the metallic *Cmca*-24 phase at 90 GPa [10].

Besides elementary substances, electrider states were reported for Al [13], Mg_3O_2 [14], Na_3Cl [15], and Na_2He [16], SiO [17]. Many of these compounds have chemical formulas very different from those known at zero pressure.

The Effect of Core Electron and Anti-Wilson Phase Transition

The free electron gas model is a convenient tool to show the expected effect of band broadening under pressure. Besides being convenient, this model becomes exact (if one neglects nuclear strong and weak interactions) for any chemical system at infinite compression. In this model, the electronic dispersion relation is $E_k = \hbar^2 k^2 / 2m$. Here, the wave vector is in the momentum space, $k \in (-\pi/a, \pi/a)$, where a is the lattice parameter. So the band width $\Delta E_k = \hbar^2 \pi^2 / 2ma^2$. With pressure reducing the lattice parameter, the range of both k and ΔE will increase, which is ruled by Heisenberg's uncertainty principle. This means that in this simple theoretical model, Heisenberg's uncertainty principle requires that the band width of solids increases with pressure.

For a semiconductor or insulator at high pressure, the broadening band will occupy the energy space of forbidden band, thereby decreasing the band gap. If the pressure is sufficiently high, the conduction band and valence band will finally overlap, and the insulator-metal transition will occur, see Fig. 6.4. This mechanism was discovered by Wilson, after whom it is named [18].

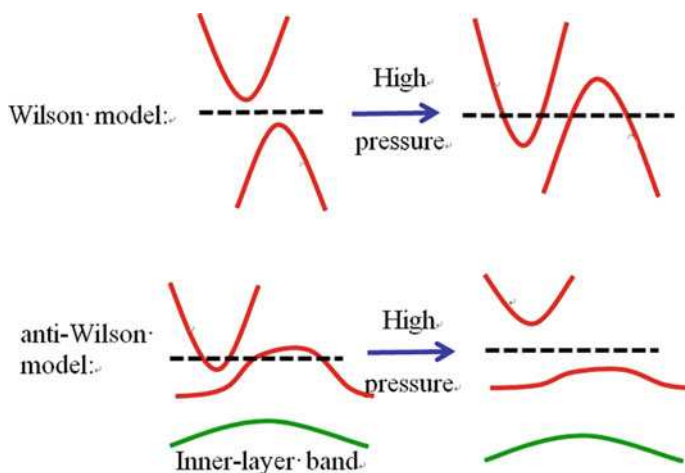


Fig. 6.4 Evolution of the band structure under pressure in Wilson and anti-Wilson models

The band overlap originating from the Wilson mechanism affects the electronic states near Fermi surface, and is normally accompanied with the strengthening of electron–phonon coupling to cause the Peierls distortion, or other more complex phonon and electron effects, often causing complex phase transitions. The related pressure-induced insulator–metal phase transition is usually called the Wilson transition.

Wilson transition is indeed a common phenomenon at high pressure, but based on a crude theoretical model of free electron gas, which ignores the effect of atomic cores—i.e., strong Pauli and electrostatic repulsion of valence electrons from the core orbitals. In quantum mechanics, valence orbitals must be radially orthogonal with core electrons of the same angular momentum—and can be thought to be not “allowed” to get close to the core due to the Pauli exclusion principle. If pressure is sufficiently high, most of the free volume for such electrons will disappear and such “expelled” electrons will have to localize in the interstitial space. This should be accompanied by band narrowing—instead of band broadening, i.e., exactly opposite to the Wilson model. As a result, with pressure increasing, one can often observe the transformation of the initial metallic state into a poor metal with a decreased density of states (DOS) at the Fermi level (N_F), such as *t*/19-Na [19] and CaLi₂ [20] or opening of the band gap, as in elemental Na [8] and Li [10]. However, at sufficiently high pressures a reentrant metallization must occur: for example, Li and Na become metal again at 95 GPa [10] and 15.5 TPa [21], respectively. At pressures of order of 1 a.u. (29.4 TPa), we expect the disappearance of the periodic law, which will be replaced with the physics of the free electron gas to govern the behavior of all compounds. At further compression, when the internuclear distances become much smaller than the electronic de Broglie wavelength, electrons stop feeling nuclear attraction—this is what happens in white dwarfs (pressures of order 10²² Pa) [22].

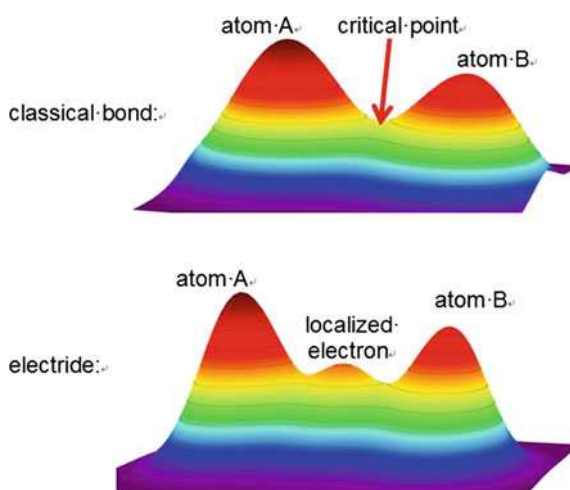
Physical Form: Duality of Pseudoatoms and Multicenter Bonds

Pseudoatoms

In classical crystal chemistry, there are four main types of bonding: covalent, metallic, ionic, and van der Waals. Bader theory [23] is one of the ways to describe bonding quantitatively. Electronic charge density $\rho(x, y, z)$ is continuous throughout the space, and has stationary points with $\partial\rho/\partial x = \partial\rho/\partial y = \partial\rho/\partial z = 0$, i.e., $\nabla\rho = 0$. Considering second derivatives, density minima have $\partial^2\rho/\partial x^2, \partial^2\rho/\partial y^2, \partial^2\rho/\partial z^2 > 0$, and maxima have negative second derivatives (and maxima coincide with the positions of the nuclei—although in a static picture, density maxima at nuclei have a cusp, rather than zero derivative of the density). Saddle points, called bond critical points in Bader theory, can have negative Laplacian ($\nabla^2\rho < 0$) when the electrons are locally concentrated and shared by both nuclei (usually implying covalent interactions) or positive Laplacian (i.e., $\nabla^2\rho > 0$) when the electrons are concentrated around the atoms (implying closed-shell interactions).

However, for electriles a different picture emerges: they display significant charge density maxima not corresponding to positions of nuclei, as shown in Figs. 6.2a, 6.5 and 6.6a. This implies that electronic concentration in electriles is much stronger than in a normal covalent bond and even reverses the sign of the second derivative to create a local maximum without a nucleus. The effect of electron concentration can be clearly seen also in the deformation charge density [24] and electron localization function (ELF) [25]. Deformation charge density is the difference between the actual charge density and superposition of non-interacting atomic charge densities. As shown in Fig. 6.6b, interstitial voids get the greatest increase of electron density—

Fig. 6.5 Electronic charge density in a normal bond and in an electrile



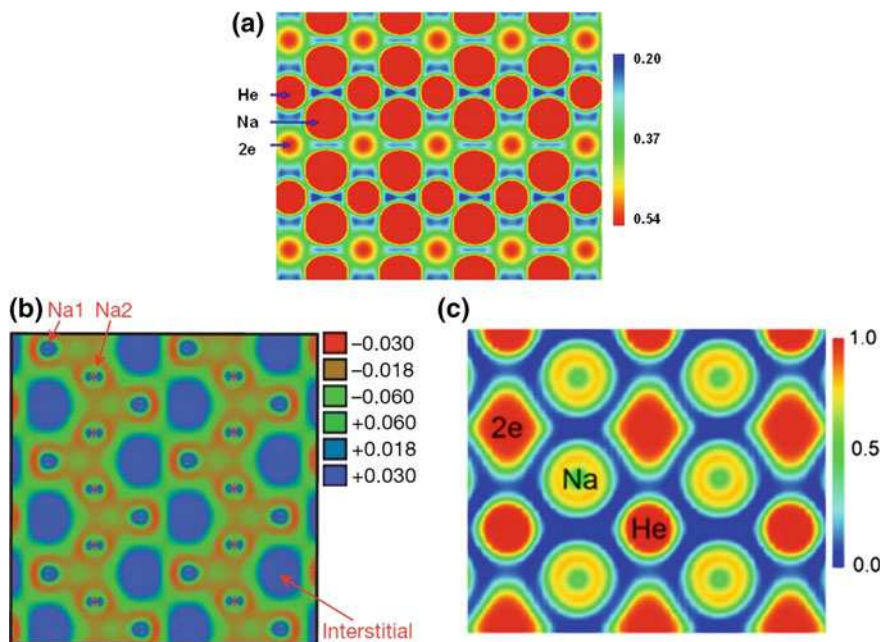


Fig. 6.6 **a** Computed charge density ($e \text{ \AA}^{-3}$) of Na_2He at 300 GPa, plotted in the [110] plane of the conventional cell [16]. **b** Deformation charge density of *hP4*-Na plotted in the [110] plane [8]. **c** ELF of Na_2He in the [110] plane [16]

in other words, when an electride state is formed, valence electrons concentrate in the interstitial space. ELF distributions give a similar picture. ELF is defined in the range [0, 1], with $\text{ELF} = 1$ corresponding to perfect localization, and $\text{ELF} = 0.5$ to electron gas. In the electride Na_2He (Fig. 6.6c), the interstitial electron has almost $\text{ELF} = 1$, even higher than for the core $2s$ and $2p$ electrons of Na.

There are rather many elemental solids and compounds which have nonnuclear charge density maxima. Only some of them have band gaps, while others are metals. In metals, electron gas very effectively screens long-range electrostatic interactions. Whether the system is metallic or not, depends on the height of the potential barrier and the ability of the electrons to tunnel through it. For example, *d*-electrons penetrate the core regions of K, Rb, and Cs, while core radius is too small to isolate the localized electrons in some Li compounds such as Li_6O . A proper distinction would be between: (1) strong electrides (such as Na, Li, and Mg_3O_2), defined as insulators or semiconductors with localized electrons playing the role of an anion in an ionic crystal. (2) weak electrides (such as K, Ca, Mg, Al, Li_6O), defined as metallic systems with non-nuclear charge density maxima.

The electricle state has been proven in many compounds and the origin of its stability is interesting to explore. In quantum mechanics, without nuclear attraction, electronic wave function will delocalize throughout the entire space. This is obviously in conflict with the charge density distributions observed in electricles. To reconcile this contradiction, we add a volumetric constraint in the quantum system, and discover another picture, quite different from the electron gas model. Here we use a simplified wave packet model.

Related to the uncertainty principle, there is the Robertson-Schrödinger inequality,

$$\langle A^2 \rangle \langle B^2 \rangle \geq \frac{1}{4} |\langle [A, B] \rangle|^2, \quad (6.2)$$

so

$$\langle i^2 \rangle \langle p_i^2 \rangle \geq \frac{\hbar^2}{4}, \quad i = x, y, z, \quad (6.3)$$

where p_x, p_y, p_z is the momentum of the particle, and $\langle \bar{x} \rangle = \langle \bar{y} \rangle = \langle \bar{z} \rangle = 0$, $\langle \bar{p}_x \rangle = \langle \bar{p}_y \rangle = \langle \bar{p}_z \rangle = 0$.

If the particle is localized with a volumetric constraint, then

$$\langle x^2 \rangle \langle y^2 \rangle \langle z^2 \rangle \leq V, \quad (6.4)$$

where V is a constant, which means the wave function cannot extend infinitely. So the kinetic energy is

$$\begin{aligned} E_k &= \frac{1}{2m} (\langle p_x^2 \rangle + \langle p_y^2 \rangle + \langle p_z^2 \rangle) \\ &\geq \frac{3}{2m} \sqrt[3]{\langle p_x^2 \rangle \langle p_y^2 \rangle \langle p_z^2 \rangle} \\ &\geq \frac{3\hbar^2}{8m} (\langle p_x^2 \rangle \langle p_y^2 \rangle \langle p_z^2 \rangle)^{-1/3} \\ &\geq \frac{3\hbar^2}{8m} V^{-1/3}. \end{aligned} \quad (6.5)$$

If and only if $\langle p_x^2 \rangle = \langle p_y^2 \rangle = \langle p_z^2 \rangle$ (spherically symmetric localization), and $\langle i^2 \rangle \langle p_i^2 \rangle = \hbar^2/4$ ($i = x, y, z$) (Gaussian wave packet), the kinetic energy reaches its minimum. Next, we take a Gaussian wave packet as an example. We assume that the wave packet has anisotropy, which means it is an ellipsoid with A, B, C as its principal axes, where $A = 1/2\langle x^2 \rangle$, $B = 1/2\langle y^2 \rangle$, $C = 1/2\langle z^2 \rangle$. So, its wave function is

$$\varphi(x, y, z) = \left(\frac{ABC}{\pi^3} \right)^{1/4} e^{-\frac{1}{2}(Ax^2 + By^2 + Cz^2)}, \quad (6.6)$$

and its kinetic energy is

$$\begin{aligned}
 E_k &= \langle \varphi | E | \varphi \rangle = -\frac{\hbar^2}{2m} \int \varphi^* \nabla^2 \varphi \, dx dy dz \\
 &= \frac{\hbar^2}{4m} (A + B + C) \\
 &\geq \frac{3\hbar^2}{4m} (ABC)^{1/3} \\
 &= \frac{3\hbar^2}{8m} (\langle x^2 \rangle \langle y^2 \rangle \langle z^2 \rangle)^{-1/3}.
 \end{aligned} \tag{6.7}$$

Only if $A = B = C$, the inequality becomes an equality.

In simple words, if there is a limited volume available to the electron, Heisenberg's uncertainty principle requires an increased uncertainty in the momentum space, increasing the kinetic energy of the electron and leading to its localization as a spherical Gaussian wave packet (to decrease this kinetic energy). In a word, volumetric constraint and uncertainty principle are the driving forces behind the formation of nonnuclear charge density maxima, characteristic of electrides.

With the localization as spherical Gaussian wave packets, such bare electrons will behave as atomic particles—anions—and we can consider them as independent particles. Compared to true atoms with central potentials from nucleus attraction, interstitial electrons are compressible and easy to reshape. At high pressure, interstitial electrons are usually spin-paired, which often means that an electron pair occupies one interstitial area. It has a radius somewhat smaller than He atom, which also contains one electron pair. For example, in Na_2He compound, the radius of $2e$ is about 0.9 of the radius of He.

Considering the interstitially localized electrons as pseudoatoms, we can evaluate their interaction with cations and other anions. Normally, electrides have structures similar to either alloys or ionic phases: for example, $hP4\text{-Na}$ has the Ni_2In structure, where Na atoms occupy the positions of Ni atoms and interstitial electrons occupy the In sites. The $hP4$ structure can be viewed as a strongly (\sim twofold) squeezed along the c -axis double hexagonal close packing ($\dots ABAC \dots$) of Na atoms, or as a nearly perfect hexagonal close packing of the localized electrons. This implies that interstitial electrons have a nearly isotropic interaction, leading to close-packed structure in this and other examples.

In 2014, Miao and Hoffmann [26] discovered a method to calculate the orbital energies in atoms under pressure: they used a sufficiently large ($3 \times 3 \times 3$) supercell of the perfect He fcc structure relaxed at a given pressure, where they consider He as a chemically inert space filler and pressure transmitting medium. In that supercell, they replaced the central He atom by the atom of interest, relaxed the structure, and computed its electronic DOS. Assuming the highest occupied molecular orbital (HOMO) of the helium matrix fixed, irrespective of the inserted atom, one can get the relative orbital energies at high pressure. Considering localized electrons as a new

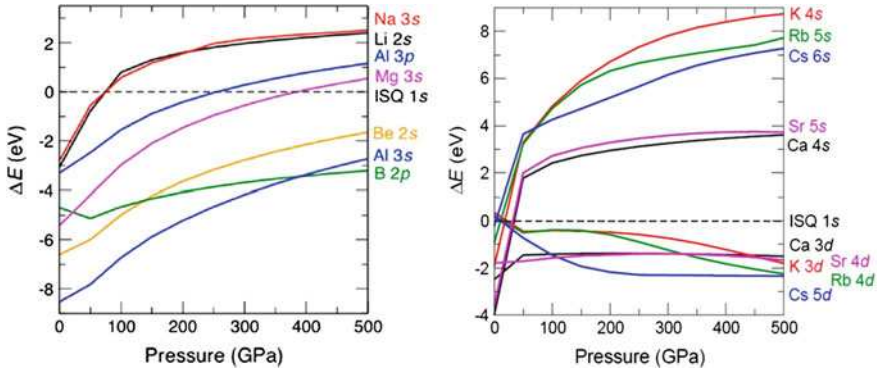


Fig. 6.7 Orbital energy of an electron on the corresponding orbital [26]. ISQ stands for “interstitial quasi-atom”, which is set as reference zero energy

type of element, they also replaced the central He atom with an additional electron to represent the electriles.

Using the He matrix method described above, one can get the orbital energies of different elements (Fig. 6.7). At hundreds of GPa, the highest occupied orbitals of Na, Li, Al, and Mg exceed the orbital level of interstitial electrons, which means the donation of electrons to the interstices is energetically favorable.

For heavier alkali metals, such as K, Rb, and Cs, high-pressure behavior is quite different from light alkalis Li and Na. The difference comes from d -orbital effects and s - d transfer [27]. At zero pressure, n s -orbitals with $n - 1$ nodes have lower energy than $(n - 1)$ d -orbitals with $(n - 3)$ nodes, but at high pressure, $(n - 1)$ d -orbitals become energetically more favorable and become occupied. So, the n s -electron will transfer to the $(n - 1)$ d -orbital, making heavy alkali metals effectively transition metals under pressure and, in some way, rearranging the Periodic Table [22]. For example, the electronic configuration of K changes from $[\text{Ar}]4s^1$ to $[\text{Ar}]3d^1$. Additionally, with less Pauli exclusion from core electrons than ns electrons, $(n - 1)$ d -electrons are more localized in the core and easier to tunnel the energy barrier formed by overlapped core electrons at high pressure. As a result, at high pressure, K, Rb, and Cs, although they do have (diminished) nonnuclear charge density maxima, are metallic. The core localization of d -electrons and s - d transfer also lead to changes in the chemical activity under pressure. This s - d transfer happens easily in K and heavier alkalis: $4s$ - $3d$ orbital transition requires moderate energy, whereas in Na the $3s$ - $3d$ transition is energetically very costly and s - d transition is never complete (even more so in Li). So the light active elements, such as Li, Na, very easily adopt the electrile state and can form semiconducting and insulating phases at high pressure, but K, Rb and Cs cannot.

Multicenter Bonds

In the above picture of valence electrons being “squeezed out” by core electrons, the interatomic distances should be sufficiently small—smaller than the sum of the core radius of one atom and valence orbital radius of the other. For example, the shortest Na–Na distance in *hP4*-Na is 1.89 Å at 300 GPa, and the 3*s* orbital radius of Na is 1.71 Å, whereas the size of the core is best modeled by the ionic radius of Na⁺ (1.02 Å). This indicates a strong core–valence overlap and core–core overlap. Due to short distances from nonnuclear density maxima to neighboring atoms, these localized electrons can be considered as a multicenter bond formed at high pressure—however, this description seems even more appropriate in those cases where interatomic distances are longer than sum of core and valence radii (for example, in the high-pressure compound SiO [17]).

Here we use a simplified model, Na₈ cluster, to investigate this idea. Put eight Na atoms in the vertices of a cube, then we get a Na₈ cluster with symmetry group *O_h*. We set *a* as the edge length, which is also the shortest bond length in the Na₈ cluster. Every Na atom has 1 valence electron on the 3*s* orbital and Na₈ cluster has eight valence electrons and four new hybridized bonding orbitals. Because of the high symmetry of *O_h* group, these four orbitals can be represented as 1 *a_{1g}* orbital and 3 triply degenerated *t_{1u}* orbitals. Specifically, the *a_{1g}* orbital is nearly spherical and has *s*-wave symmetry, while the *t_{1u}* orbital has *p*-wave symmetry. The whole Na₈ cluster is a quantum dot and behaves like a superatom.

With the bond length corresponding to atmospheric pressure, *a* = 3.7 Å, the wave function is quite flat (around 0.025 a.u.) and its maximum is near the surface of cube, as shown in Fig. 6.8a, b and e. It means that the electrons delocalize in the space, displaying an electron gas-like behavior. However, when we compress the cube to *a* = 2.0 Å (the ionic radius of Na⁺ is 1.02 Å, i.e., there is now some core-core overlap), the wave functions are quite different. For *a_{1g}* orbital, the charge density maximum moves to the cube center, with an obviously strong concentration of the wave function. This orbital can be seen as an eight-center two-electron (8*c*-2*e*) bonds, because two electrons occupy this orbital and are shared by eight nuclei. For *t_{1u}* orbitals, the Na₈ cluster is more like a single atom with *p*-wave than that with *a* = 3.7 Å. The charge density is now concentrated far outside the Na₈ cube, and can be thought to be suitable for forming bonds with outside entities, while the 8*c*-2*e* bond stabilizes the cluster itself.

Now we can expand this simplified model into a true system, Na₂He, formed at high pressure (>113 GPa) [16]. The structure of Na₂He belongs to the very dense Heusler alloy structure (AlCu₂Mn-type, related to Fe₃Al-type): He atoms form a cubic close packing, in which all tetrahedral voids are filled by Na atoms, and 2*e* fill all octahedral voids. Every He atom (and every 2*e*) is coordinated by eight Na atoms. Note that 2*e* form a cubic close packing of their own—just like in *hP4*-Na, where they form a nearly perfect hexagonal close packing. In this geometry, localized electrons are inside the Na₈ cluster and occupy the *a_{1g}* orbitals. Every Na has *sp*³-hybridization and participates in four 8*c*-2*e* bonds. The hybridization of Na and the existence of 8*c*-2*c* bonds is proven by solid-state adaptive natural density

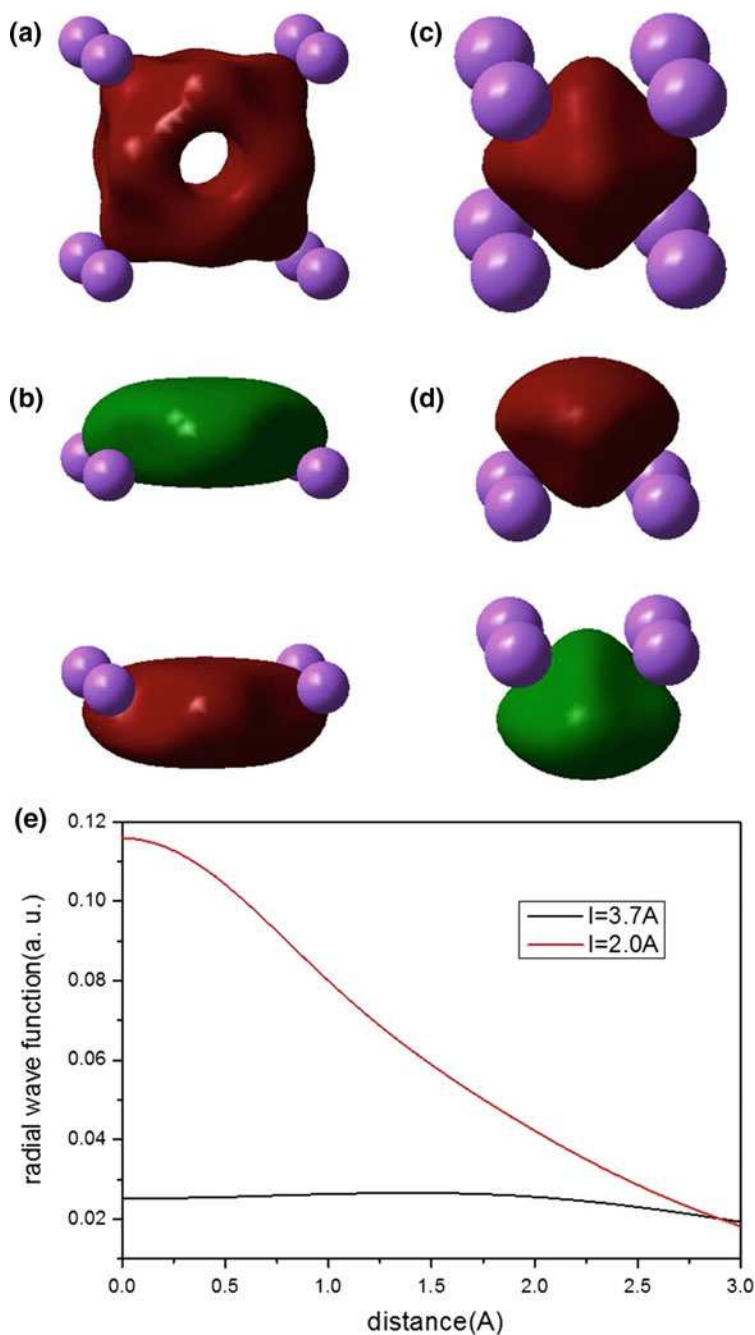


Fig. 6.8 Orbital wave functions of Na₈ cluster. ℓ is the edge length of Na₈ cube. **a** the a_{1g} orbital with cube side $a = 3.7 \text{ \AA}$. **b** the t_{1u} orbital with $a = 3.7 \text{ \AA}$. **c** the a_{1g} orbital with $a = 2.0 \text{ \AA}$. **d** the t_{1u} orbital with $a = 2.0 \text{ \AA}$. **e** the radial wave function as a function of the distance from cube center for $a = 3.7 \text{ \AA}$ and 2.0 \AA

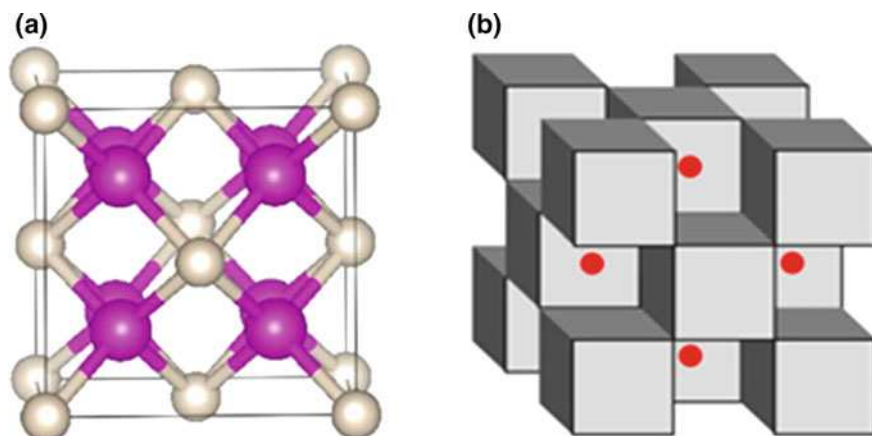


Fig. 6.9 Crystal structure of Na_2He at 300 GPa. **a** ball-and-stick representation (*pink* and *gray* atoms represent Na and He, respectively) and **b** polyhedral representation, where half of Na_8 cubes are centered by He atoms (shown by polyhedra), and half by $2e$ (shown by *red spheres*) [16] (color figure online)

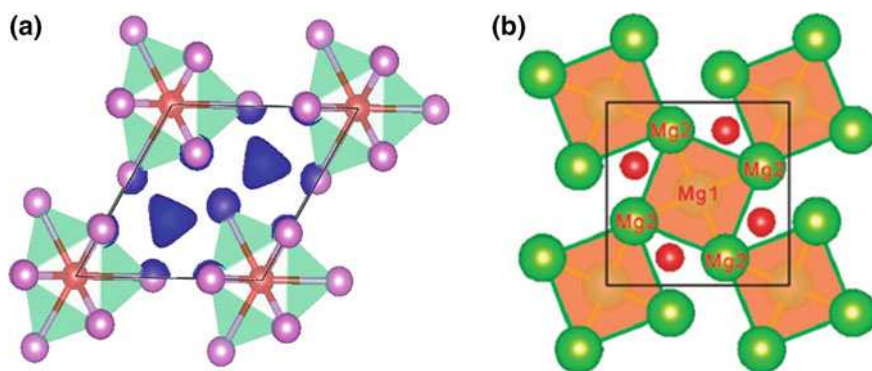


Fig. 6.10 Crystal structure of **a** Li_6O [32] with *blue* isosurface of $\text{ELF} = 0.9$ and **b** Mg_3O_2 [14]. In Mg_3O_2 , there is a strong charge density localization between four Mg_2 and two Mg_1 atoms (color figure online)

partitioning (SSAdNDP) [28, 29] and periodic natural bond orbital (NBO) methods [30, 31] (Figs. 6.9 and 6.10).

The Novel Chemistry of Electrides

The interstitially localized electrons greatly change the electronic state of the elements and compounds, leading to altered chemical properties. It is known that Dye's zero-pressure electride has very low work function and is a strong reducing agent [5]. Similarly, high-pressure electrides possess unusual chemical properties.

The first chemical phenomenon originating from the electride state is the formation of clusters of electropositive metals. Normal stoichiometries are governed by valence ratios, and once compounds have more metal atoms than prescribed by valence ratio, there must be bonds among the metal atoms: this happens in the suboxides of caesium and rubidium: Rb_9O_2 , Rb_6O , Cs_{11}O_3 , Cs_4O , Cs_7O , $\text{Cs}_{11}\text{O}_3\text{Rb}$, $\text{Cs}_{11}\text{O}_3\text{Rb}_2$, and $\text{Cs}_{11}\text{O}_3\text{Rb}_3$ [33]. It is remarkable that in these zero-pressure metal-rich compounds, big electropositive elements form a metallic framework and electronegative elements fill the interstices. Many of these are electrides.

At high pressure, smaller electropositive metals, such as Li, Na, and Mg, form metal-rich compounds, which are unknown at zero pressure. The representative cases are Li_6O [32] and Mg_3O_2 [14]. In these compounds, there is hollow space inside the clusters made of metal atoms, and these interstices are occupied by localized electrons. These metal clusters are stabilized by two factors: (1) localized electrons carry a negative charge and behave as anions, binding together the surrounding metal cations. In this way, the whole system is built by Madelung field with two different kinds of anions. (2) if we consider the localized electrons as multicenter bonds, the cluster is combined and stabilized by this electron concentration.

Another chemical peculiarity of high-pressure electrides is their likely extreme reducing ability. In fact, interstitial localization of the electrons is a compromise solution: these electrons have nowhere else to go. Once an electride is combined with other elements that have unoccupied low-energy orbitals, the electrons will move into these orbitals. Like for zero-pressure electrides, we expect very low work functions. A special feature of high-pressure electrides is their extreme chemical activity: at high pressure, one of the most inert elements, He, can receive ~ 0.1 electrons from Na [16]. We have found [22] that under pressure, Na has the lowest electronegativity (closely followed by Mg) among all elements—even lower than Cs, and this is directly related to its propensity to form the electride state.

Actually, electrides with metal clusters can be considered as normal compounds reduced by elemental electrides. For example, MgO is a saturated system with normal stoichiometry defined by the valence ratio. At high pressure, the electride Mg can reduce it: reaction $\text{Mg} + 2\text{MgO} = \text{Mg}_2\text{O}_3$ occurs at pressures above 500 GPa. In this way, the formation of metal clusters is a manifestation of the extreme reducing ability of electride.

In summary, we systematically surveyed high-pressure electrides, using theory, model systems, and real compounds, and considering the nature of their stability, as well as their physical and chemical properties. Electrides, with strongly localized interstitial electron density maxima, which can be considered as pseudoatoms or multicenter bonds, possess extreme chemical activity, reducing ability and can be used as a path to a new branch of high-pressure chemistry.

Acknowledgements This work is supported by NSAF (Grant No. U1530402), Special Program for Applied Research on Super Computation of the NSFC-Guangdong Joint Fund (the second phase), research funds of Skoltech and MIPT, and by the Foreign Talents Introduction and Academic Exchange Program (No. B08040).

References

1. J.L. Dye, *Science* **301**(5633), 607 (2003). DOI [10.1126/science.1088103](https://doi.org/10.1126/science.1088103)
2. J.S. Landers, J.L. Dye, A. Stacy, M.J. Sienko, *J. Phys. Chem.* **85**(9), 1096 (1981). DOI [10.1021/j150609a004](https://doi.org/10.1021/j150609a004)
3. S. Matsuishi, Y. Toda, M. Miyakawa, K. Hayashi, T. Kamiya, M. Hirano, I. Tanaka, H. Hosono, *Science* **301**(5633), 626 (2003). DOI [10.1126/science.1083842](https://doi.org/10.1126/science.1083842)
4. J.L. Dye, *Science* **247**(4943), 663 (1990). DOI [10.1126/science.247.4943.663](https://doi.org/10.1126/science.247.4943.663)
5. J.L. Dye, *Acc. Chem. Res.* **42**(10), 1564 (2009). DOI [10.1021/ar9000857](https://doi.org/10.1021/ar9000857)
6. B. Rousseau, N.W. Ashcroft, *Phys. Rev. Lett.* **101**, 046407 (2008). DOI [10.1103/PhysRevLett.101.046407](https://doi.org/10.1103/PhysRevLett.101.046407)
7. F. Siringo, R. Pucci, G.G.N. Angilella, *High Press. Research* **15**(4), 255 (1997). doi:[10.1080/08957959708244246](https://doi.org/10.1080/08957959708244246). Also available as preprint [arXiv.org/abs/cond-mat/9512011](https://arxiv.org/abs/cond-mat/9512011)
8. Y. Ma, M. Eremets, A.R. Oganov, Y. Xie, I. Trojan, S. Medvedev, A.O. Lyakhov, M. Valle, V. Prakapenka, *Nature* **458**, 182 (2009). DOI [10.1038/nature07786](https://doi.org/10.1038/nature07786)
9. C.L. Guillaume, E. Gregoryanz, O. Degtyareva, M.I. McMahon, M. Hanfland, S. Evans, M. Guthrie, S.V. Sinogeikin, H. Mao, *Nat. Phys.* **7**, 211 (2011). DOI [10.1038/nphys1864](https://doi.org/10.1038/nphys1864)
10. M. Marqués, M.I. McMahon, E. Gregoryanz, M. Hanfland, C.L. Guillaume, C.J. Pickard, G.J. Ackland, R.J. Nelmes, *Phys. Rev. Lett.* **106**(9), 095502 (2011). DOI [10.1103/PhysRevLett.106.095502](https://doi.org/10.1103/PhysRevLett.106.095502)
11. C.J. Pickard, R.J. Needs, *Phys. Rev. Lett.* **102**, 146401 (2009). DOI [10.1103/PhysRevLett.102.146401](https://doi.org/10.1103/PhysRevLett.102.146401)
12. J. Lv, Y. Wang, L. Zhu, Y. Ma, *Phys. Rev. Lett.* **106**(1), 015503 (2011). DOI [10.1103/PhysRevLett.106.015503](https://doi.org/10.1103/PhysRevLett.106.015503)
13. C.J. Pickard, R.J. Needs, *Nat. Mater.* **9**(8), 624 (2010). DOI [10.1038/nmat2796](https://doi.org/10.1038/nmat2796)
14. Q. Zhu, A.R. Oganov, A.O. Lyakhov, *Phys. Chem. Chem. Phys.* **15**, 7696 (2013). DOI [10.1039/C3CP50678A](https://doi.org/10.1039/C3CP50678A)
15. W. Zhang, A.R. Oganov, A.F. Goncharov, Q. Zhu, S.E. Boulfelfel, A.O. Lyakhov, E. Stavrou, M. Somayazulu, V.B. Prakapenka, Z. Konôpková, *Science* **342**(6165), 1502 (2013). DOI [10.1126/science.1244989](https://doi.org/10.1126/science.1244989)
16. X. Dong, A.R. Oganov, A.F. Goncharov, E. Stavrou, S. Lobanov, G. Saleh, G.R. Qian, Q. Zhu, C. Gatti, X.F. Zhou, V. Prakapenka, Z. Konôpková, H.T. Wang, Stable compound of helium and sodium at high pressure (2013). [arXiv:1309.3827](https://arxiv.org/abs/1309.3827)
17. H. Niu, A.R. Oganov, X.Q. Chen, D. Li, *Sci. Rep.* **5**, 18347 (2015). DOI [10.1038/srep18347](https://doi.org/10.1038/srep18347)
18. N.F. Mott, Z. Zinamon, *Rep. Progr. Phys.* **33**(3), 881 (1970). DOI [10.1088/0034-4885/33/3/302](https://doi.org/10.1088/0034-4885/33/3/302)
19. E. Gregoryanz, L.F. Lundegaard, M.I. McMahon, C. Guillaume, R.J. Nelmes, M. Mezouar, *Science* **320**, 1054 (2008). DOI [10.1126/science.1155715](https://doi.org/10.1126/science.1155715)
20. Y. Xie, A.R. Oganov, Y. Ma, *Phys. Rev. Lett.* **104**, 177005 (2010). DOI [10.1103/PhysRevLett.104.177005](https://doi.org/10.1103/PhysRevLett.104.177005)
21. Y. Li, Y. Wang, C.J. Pickard, R.J. Needs, Y. Wang, Y. Ma, *Phys. Rev. Lett.* **114**, 125501 (2015). DOI [10.1103/PhysRevLett.114.125501](https://doi.org/10.1103/PhysRevLett.114.125501)
22. X. Dong, A.R. Oganov, G. Qian, X.F. Zhou, Q. Zhu, H.T. Wang, How do chemical properties of the atoms change under pressure (2015). [arXiv:1503.00230](https://arxiv.org/abs/1503.00230)
23. R.F.W. Bader, *Atoms in Molecules: A Quantum Theory* (Oxford University Press, Oxford, 1994)
24. F.L. Hirshfeld, *Theor. Chim. Acta* **44**(2), 129 (1977). DOI [10.1007/BF00549096](https://doi.org/10.1007/BF00549096)
25. A.D. Becke, K.E. Edgecombe, *J. Chem. Phys.* **92**(9), 5397 (1990). DOI [10.1063/1.458517](https://doi.org/10.1063/1.458517)
26. M.S. Miao, R. Hoffmann, *Acc. Chem. Res.* **47**(4), 1311 (2014). DOI [10.1021/ar4002922](https://doi.org/10.1021/ar4002922)
27. M. Winzenick, V. Vijayakumar, W.B. Holzapfel, *Phys. Rev. B* **50**, 12381 (1994). DOI [10.1103/PhysRevB.50.12381](https://doi.org/10.1103/PhysRevB.50.12381)
28. T.R. Galeev, B.D. Dunnington, J.R. Schmidt, A.I. Boldyrev, *Phys. Chem. Chem. Phys.* **15**, 5022 (2013). DOI [10.1039/C3CP50350J](https://doi.org/10.1039/C3CP50350J)

29. D.Y. Zubarev, A.I. Boldyrev, *Phys. Chem. Chem. Phys.* **10**, 5207 (2008). DOI [10.1039/B804083D](https://doi.org/10.1039/B804083D)
30. B.D. Dunnington, J.R. Schmidt, *J. Chem. Theo. Comp.* **8**(6), 1902 (2012). DOI [10.1021/ct300002t](https://doi.org/10.1021/ct300002t)
31. J.P. Foster, F. Weinhold, *J. Am. Chem. Soc.* **102**(24), 7211 (1980). DOI [10.1021/ja00544a007](https://doi.org/10.1021/ja00544a007)
32. X. Dong, Y.L. Li, A.R. Oganov, K. Li, H. Zheng, H. kwang Mao, Novel chemistry of lithium oxides and superconducting low-pressure LiO₄ (2016). [arXiv:1603.02880](https://arxiv.org/abs/1603.02880)
33. A. Simon, *Coord. Chem. Rev.* **163**, 253 (1997). DOI [10.1016/S0010-8545\(97\)00013-1](https://doi.org/10.1016/S0010-8545(97)00013-1)